



DYNAMIC RESPONSES OF THE HEAD AND CERVICAL SPINE TO AXIAL IMPACT LOADING

Roger W. Nightingale, James H. McElhaney, William J. Richardson and Barry S. Myers

Duke University, Department of Biomedical Engineering, and Division of Orthopaedic Surgery, Box 90281, Durham, NC 27708-0281, U.S.A.

Abstract—This study explores the inertial effects of the head and torso on cervical spine dynamics with the specific goal of determining whether the head mass can provide a constraining cervical spine end condition. The hypothesis was tested using a low friction impact surface and a pocketing foam impact surface. Impact orientation was also varied. Tests were conducted on whole unembalmed heads and cervical spines using a drop track system to produce impact velocities on the order of 3.2 m s^{-1} . Data for the head impact forces and the reactions at T1 were recorded and the tests were also imaged at 1000 frames s^{-1} .

Injuries occurred 2–19 ms following head impact and prior to significant head motion. Average compressive load a failure was $1727 \pm 387 \text{ N}$. Decoupling was observed between the head and T1. Cervical spine loading due to head rebound constituted up to $54 \pm 16\%$ of the total axial neck load for padded impacts and up to $38 \pm 30\%$ of the total axial neck load for rigid impacts. Dynamic buckling was also observed; including first-order modes and transient higher-order modes which shifted the structure from a primarily compressive mode of deformation to various bending modes.

These experiments demonstrate that in the absence of head pocketing, the head mass can provide sufficient constraint to cause cervical spine injury. The results also show that cervical spinal injury dynamics are complex, and that a large sample size of experimentally produced injuries will be necessary to develop comprehensive neck injury models and criteria.

Keywords: Cervical spine; Injury; Impact; Dynamics; Buckling.

INTRODUCTION

In order to minimize the risk of injury to the cervical spine, some measure of injury potential is required. Although there are numerous studies on head and neck injury, a theory which considers arbitrarily directed impulses over the entire head and neck has not yet evolved. Before such a theory can be developed, additional, quantitative biomechanical data about the kinematics of head impact, and the energy absorbing capabilities and failure modes of the head and neck must be obtained.

In situations where the neck must stop the torso, the head-neck complex must either move out of the path of, or be at risk for injury from, the energy of the following torso. Therefore, constraints on head motion can influence injury risk and injury mechanism. Head constraint can arise from pocketing in the impact surface, from the active neck musculature, and from the inertia of the head itself. A number of previous studies support this hypothesis. Hodgson and Thomas (1980) suggested that restriction of motion of the atlantoaxial joint greatly increases the risk of injury. Bauze and Ardran (1978) produced bilateral facet dislocation in the cadaver by constraining the rotation of the head and inserting a peg in the neural foramen. Yoganadan *et al.* (1986) noted that constraining head motion with simulated musculature increased the number of injuries in cadaver head and neck impacts. Myers *et al.* (1991) observed large increases in axial stiffness of the cervical spine as a function of increasing constraint of the cranial end condition in quasi-static

tests. Despite the large body of literature on neck injury, there have been no studies, to our knowledge, which quantify cervical injury dynamics while including the dynamic effects of the head and torso masses. The primary purpose of this paper is; therefore, to test the hypothesis that the inertia of the head constrains head motion during dynamic cervical spine loading.

MATERIALS AND METHODS

The experimental apparatus was designed to model cervical spine trauma due to head impact with a following torso. A drop track system was developed incorporating a steel carriage mounted on two linear bearing sliders (Fig. 1). The specimen preparations were rigidly mounted to a 6-axis GSE 6607-00 load cell in an inverted posture, and the initial positions of the head and neck were set and maintained using a suspension frame. The effective torso mass for all tests was 16 kg. This value is an estimate of the fraction of the torso mass which acts on the neck during dynamic injury. It was generated using the GEBO software and represents the upper torso mass of the 50th percentile male. A Kistler 9067 3-axis piezoelectric load cell was used to measure the head impact forces. Acceleration transducers included a PCB 302A02 accelerometer to measure torso acceleration, and two PCB 306A06 triaxial accelerometers on the head to quantify sagittal plane head kinematics. An MTS optical sensor was used to record the impact velocity. All transducer outputs were sampled at 62.5 kHz using a PC-based digital data acquisition system. Each impact test was imaged using a Kodak Ektapro EM-2 digital camera

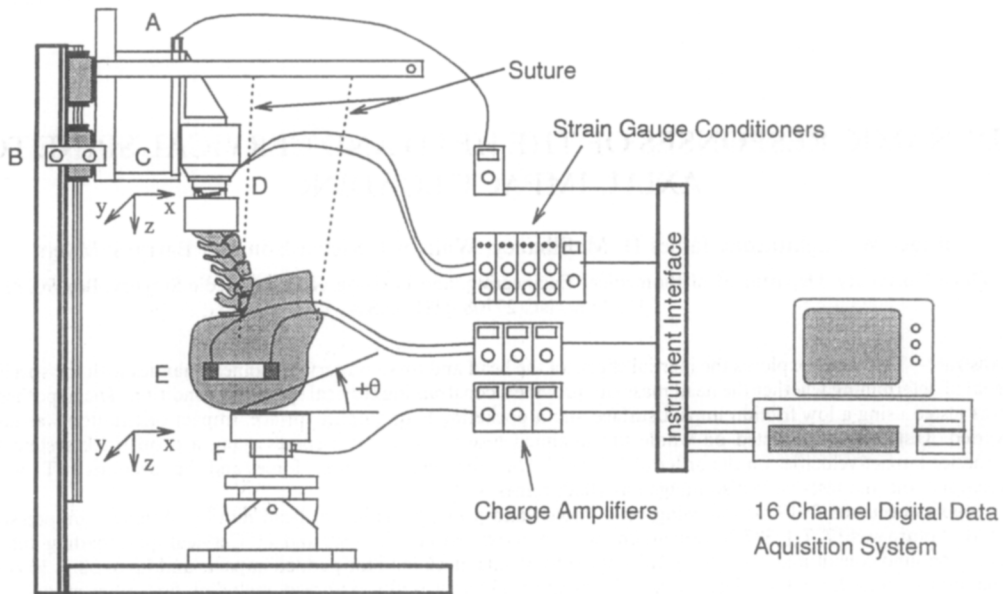


Fig. 1. A diagram of the test apparatus showing. (C) the carriage, torso mass, and linear bearing sliders. (F) the impact surface and 3-axis load cell, (D) the 6-axis GSE load cell, and (E) the head accelerometer array. The position of the torso mass was chosen as a matter of convenience. Since the thoracic vertebrae are rigidly secured to the cart and constrained to linear (vertical) motion, the position of the mass has no affect on the results. Rigid constraint on the motion of the thoracic vertebrae is necessary to accurately determine the forces and moments at the T1 level.

at 1000 frames per second. A flat steel plate measuring 15.25 cm in diameter and 4 cm in thickness was used as an impact surface. It was mounted on a locking clevis which allowed variation of the incident impact angle about the *y* axis (normal to the sagittal plane). The clevis was attached to a 42 kg steel plate using rail clamps which allowed *x* axis positioning. The plate was mounted to a structural floor and was mechanically isolated from the drop track. For rigid head impacts, the surface was covered with 3 mm of Teflon sheet to minimize friction, and for padded impacts, foams were attached using duct tape.

Eleven tests were conducted on unembalmed human heads with intact spines (Table 1). These were obtained shortly after death, sprayed with calcium buffered isotonic saline, sealed in plastic bags, frozen and stored at -20°C . All specimen handling was performed in compliance with CDC guidelines (Cavanaugh and King, 1990). During specimen harvest, the muscular tissues were removed and all ligamentous structures were kept intact, with the exception of the ligamentum nuchae. Medical records of donors were examined to ensure that the specimens were free of serious degenerative disease, spinal pathology, or other health related problems that could affect their structural responses.

Prior to testing, each specimen was transected at T3-T4 and thawed in a 100% relative chamber. Specimen preparation was also performed in a humidified chamber. The bottom two thoracic vertebrae of each specimen were cast into aluminium cups with reinforced polyester resin. The most rostral uncast vertebra was free of the resin and had a full range of motion. The C7-T1

intervertebral disk was oriented at $+25^{\circ}$ to the transverse plane to preserve the resting lordosis of the cervical spine. Photoabsorptive pins (4 mm diameter) were inserted into the anterior vertebral body, the pars interarticularis, and the spinous process of C2-C7.

A strip of scalp was removed from the parietal bone, superior to the parieto-mastoid suture and posterior to the coronal suture to install an accelerometer array. The head was mounted in an alignment frame, and a drill jig was used to make holes normal to the mid-sagittal plane. The accelerometer array was attached to the skull on a bed of dental acrylic using bone screws. The position of the array relative to the Frankfort anatomical plane was determined radiographically using lead pellets inserted into the auditory meati and the infra-orbital foraminae.

Tests were conducted using two contact surfaces. An unconstrained head end condition was simulated by a rigid steel surface covered with a 3 mm sheet of lubricated teflon ($n = 7$). The remaining tests ($n = 4$) used a more constrained head end condition which was either an expanded polystyrene foam (EPS) ($E = 2096.1 \text{ kPa}$, $\sigma_y = 206.2 \text{ kPa}$, $\rho = 0.0284 \text{ g cm}^{-3}$) or a less stiff, open cell polyurethane foam (PU) ($E = 158.6 \text{ kPa}$, $\sigma_y = 7.0 \text{ kPa}$, $\rho = 0.0277 \text{ g cm}^{-3}$). The angle of the impact surface was varied between -15° (posterior head impact) and $+30^{\circ}$ (anterior head impact).

The specimen preparations were mounted to the carriage and positioned in an anatomically neutral position. Sutures were passed through the ear lobules and the nasal septum and tied to the suspension frame to support the weight of the head and to maintain the neutral posture of the cervical spine. The preparation was raised

Table 1. Subject data, injuries, and classification

Test	Subject and initial conditions			Injury*			Cervical spine injury and classification†	HM‡
	Age/ sex	Velocity (m s ⁻¹)	Foam	Angle (deg.)	Force (N)	Time (ms)		
A	65WM	2.43§	—	0	—	—	None	Flx
B	62WM	3.20	—	0	— 1839	2.2	C1 2 part fx. through the posterior ring (CE), C2 Hangmans fx. (DE)	Flx
C	71WM	3.26	—	0	— 1955	6.5	C1 3 part comminuted fx. (VC)	Flx
D	55WM	3.14	—	— 15	—	—	Scalp laceration	Flx
E	35WF	3.28	—	— 15	—	—	None	Flx
F	— WM	3.26	—	15	— 1863	6.4	Basilar skull fx., C1 lateral mass fx. (VC), C2 Hangmans fx. (DE) C2–C3 ant. disc tear and ALL tear (DES1), C6–C7 perched bilateral facet dislocation (DFS3)	Ext
G	36WM	3.23	—	30	— 1552	8.3	C3 burst fx. (VCS3) C3–C4 ant. disc tear and ALL tear (DES1) C4–C5 ALL tear (DES1)	Ext
H	61WM	3.13	EPS	30	— 1632	14.8	C1 anterior ring fx. (CF), C4 spinous process fx. (CES1) C5 spinous process fx. (CES1) C5–C6 ant. disc tear, ALL tear, left capsular lig. (DES2)	Ext
I	46WM	3.03	PU	30	—	—	None	Ext
J	46WM	3.51	PU	30	— 2240	18.7	C1 2 part right aspect fx. (VC), C3–C4 ant. disc tear, ALL tear (DES1), C4–C5 ant. disc tear, ALL tear (DES1) C5 superior body chip avul. (DES1)	Ext
K	42WF	3.07	PU	— 15	— 1011	18.8	C2–C3 ant. disc tear, ALL tear, C2 chip (DES1) C3–C4 ant. disc tear, ALL tear, C3 chip (DES1)	Flx

* The time of occurrence and axial load for the first injury.

† Lower cervical spine injury classifications were developed by Allen *et al.* (1982). CF—compressive flexion, CE—compressive extension, VC—vertical compression, DF—distractive flexion, DE—distractive extension. S1, S2 and S3 are severity indices.

‡ Large head motion — flexion (Flx) or extension (Ext).

§ Dropped from a lower height (0.33 m).

|| Test J was released from a greater drop height (0.63 m) due to an error in experimental protocol.

into position and the cervical spine was pre-conditioned by manually exercising the neck through 60° of combined flexion and extension for fifty cycles (McElhaney *et al.*, 1983a). Nine of 11 tests had a drop height of 0.53 m, one had a drop height of 0.33 m and one had a drop height of 0.63 m. These heights were less than that required to produce skull fracture but sufficient to cause cervical spine failure (McElhaney *et al.*, 1979). After the impact, anteroposterior and lateral radiographs were taken and the heads were disarticulated at O–Cl and weighed. Injuries to both the heads and cervical spines were documented by dissection.

To measure inertial head loading and to evaluate head injury risk, the linear and angular accelerations of the head center of gravity were determined. Planar rigid

body accelerations were measured using sagittal plane components of two triaxial accelerometers mounted on the head (Fig. 2). The out of plane accelerometers were used to verify that the out-of-sagittal-plane motions (y-axis) were small. The angular accelerations and velocities were computed directly from:

$$\alpha_y = \frac{(a_{A2z} - a_{A1z})}{R_{12}}, \quad \omega_y = \sqrt{\frac{a_{A2z} - a_{A1z}}{R_{12}}}. \quad (1)$$

The x and z components of linear acceleration for the center of gravity of the head were determined from the equations for relative acceleration:

$$a_{CG_x} = a_{A1x} + R_{1CG_x} \alpha_y - R_{1CG_x} \omega_y^2, \quad (2)$$

$$a_{CG_z} = a_{A1z} - R_{1CG_z} \alpha_y - R_{1CG_z} \omega_y^2, \quad (3)$$

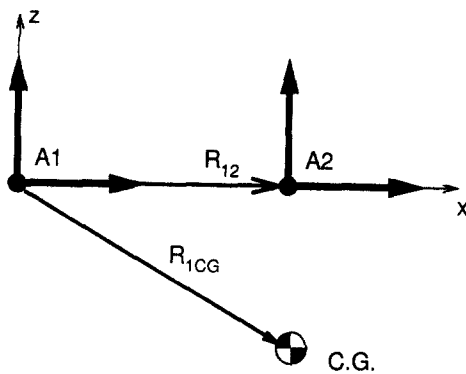


Fig. 2. The linear array used to measure sagittal plane head accelerations. The bold vectors indicate accelerometer positions and orientations. A1 is the more posterior accelerometer, and R_{1CG} locates the head center of gravity relative to accelerometer coordinate system.

where R_{1CG} is the position vector of the center of gravity relative to the location of accelerometer A1. The location of the center of gravity for each head was determined using a two-point suspension technique, and the mass moments of inertia about the center of gravity were determined using methods outlined by Walker *et al.* (1973).

All transducer data were uploaded to a Sun SparcStation 2 for analysis. Digital filtration was performed in compliance with the Society of Automotive Engineers standard for head and neck impacts (SAE J211b class 1000). Head momentum was calculated by multiplying the head mass by the impact velocity, and head impulse was calculated by integrating the first mode of the head force (see Results). Moments at the center of the C7-T1 disc were estimated using the following expression (Fig. 3):

$$M_{T1} = M + VB - PA. \quad (4)$$

The occurrence of injury was determined by a decrease in axial load with increasing cervical spine deformation (the traditional definition of failure). In contrast to quasi-static testing with the well-defined end conditions, this failure characteristic can have a number of causes in a dynamic test. Therefore, several criteria were established before it was attributed to injury. The head acceleration history and high-speed video were examined to determine if the drop in axial load was due to slip of the head on the impact surface. Video images of the cervical spine and load cell data were examined to ensure that the potential injury was not due to buckling (see Results). Finally, high-speed video, and load cell data were compared to ensure a temporal correlation between local increases in deformation and decreases in axial load at failure.

RESULTS

Cervical spine injury occurred in seven of the drops performed (Table 1) with a mean axial neck force

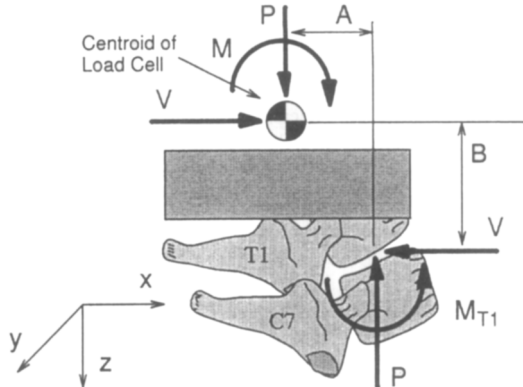


Fig. 3. A free body diagram of the load cell reactions, including the sign conventions used for data reduction and analysis. The dimensions A and B locate the geometric center of the C7-T1 intervertebral disc. To determine A and B, disc measurements were made during dissection and the location of the centroid was estimated. The values were then calculated from the images with a known dimension (casting cup diameter) in the plane of view. The anterior annulus and the disc angle are the anatomical references used in this calculation.

of -1727 ± 387 N (mean \pm S.D.). In the context of this paper, an axial force is defined as one directed in the superior-inferior (or z) direction. For the rigid impacts, the time interval for injury was 2–8 ms following head contact and for the padded impacts, the injury interval was between 14 and 19 ms. All of the injuries were associated with very little concomitant head motion. The more dramatic head motions (defined here as flexion or extension rotations $> 20^\circ$) did not occur until 22–100 ms after the impact. In all the drops, maximum head displacements, on the order of 90° in flexion or extension, occurred more than 90 ms after impact and gross motions of the head and neck were complete after 155–300 ms. In the latter portion of the $+30^\circ$ frontal impacts, the head motions involved head extension rotation as the head translated posteriorly and was arrested by the cervical spine. For all other surface orientations, the head translated anteriorly, resulting in head (and subsequent cervical spine) flexion.

No cervical spine injuries were produced in either of the rigid impacts with an impact surface orientation of -15° (posterior head impacts, tests D and E). In both of these tests the head and neck were able to escape in flexion and anterior translation. In contrast, a specimen (K) impacting a padded surface with the same orientation was unable to escape and sustained distractive extension injuries.

The dynamics of the test can be separated into a bimodal response as defined by local maxima in the head force histories (Figs 4 and 5). For the rigid impacts, Mode 1 is attributed almost entirely to stopping the head and had a duration of 4.3 ± 1.6 ms. During the first half of this mode, the head impact force reached a maximum with no concomitant neck force (Fig. 4). Neck loading at T1 was not observed until the latter half of Mode 1. For the padded impacts, the head contact times during Mode

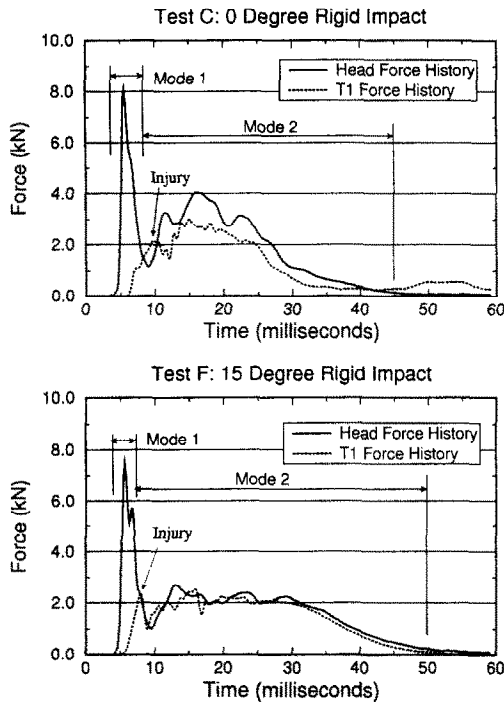


Fig. 4. Magnitudes of the resultant head and neck forces for two rigid impacts. Mode 1 of the head response is associated with stopping the head. Mode 2 is inertial loading of the head and cervical spine by the torso mass. Note the time lag between the onset of head forces and onset of cervical spine forces.

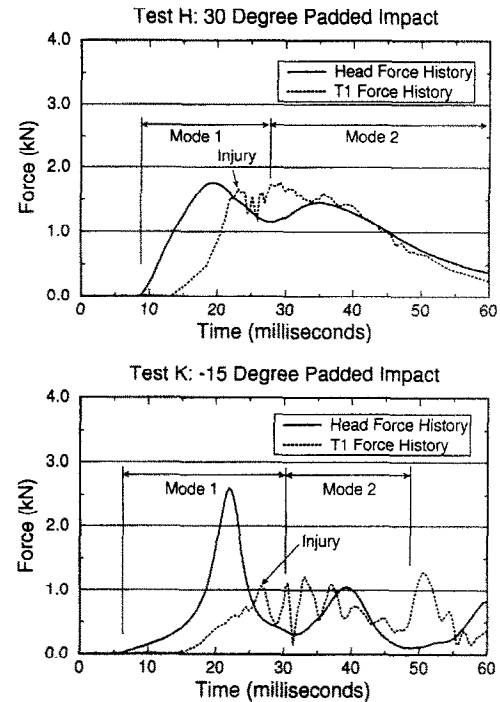


Fig. 5. Magnitudes of the resultant head and neck forces for two padded impacts. The peak head forces are significantly lower than those for the rigid impacts in Fig. 4. The head modes are not as well separated as in the rigid impacts and the time interval between the onset of head forces and onset of cervical spine forces is longer. As a result, the T1 force contributes significantly to the peak head force. Note that the neck forces are greater than the head forces during injury. This is a consequence of head rebound.

1 were significantly increased (Fig. 5). Therefore, the first mode reflects loading by the torso in addition to the force required to stop the head. The inertia of the torso mass contributed significantly to the peak head force (10–35% of the peak head force). However, the peak head force was significantly lower for the padded impacts (2961 ± 968 N) than for the rigid impacts (8306 ± 1796 N). Mode durations for the padded impacts could not be calculated because the increased coupling of the head and cervical spine resulted in less separation between modes. For both impact surfaces, Mode 2 represents head and cervical spine loading by the inertial force of the effective torso mass. The duration of Mode 2 for the rigid impact was 27.3 ± 14.3 ms.

In all the tests there was a delay in the onset of measured neck load with respect to the head load. This lag in response at T1 was 1.7 ± 0.3 ms for the rigid impacts and 6.9 ± 1.7 ms for the padded impacts (Figs 4 and 5, and Table 2). The lag is evidence that the head and cervical spine are not coupled during the first half of Mode 1. It is also evident for the rigid impacts (Fig. 4) that the inertial force exerted by the torso on the head and neck during the second half of Mode 1 is small (2–10% of the impulse) relative to the measured head force. This allows the calculation of a vertical impulse on the head by integrating Mode 1 of the z head force (Table 2). This technique could not be used to calculate head impulses for the padded impacts because the head

and torso become more coupled due to the increased duration of the head impact.

Head rebound in the vertical ($-z$) direction accounted for a significant portion of the compressive neck loading during the injury interval. From the impulse-momentum relation, it is clear that a negative vertical impulse on the head with a magnitude greater than the head momentum results in a rebound velocity [negative value of v in equation (5)]:

$$mv = \int_0^t F dt + mv_0. \quad (5)$$

This result was observed in all the impacts (rigid) where it was possible to compute a head impulse (Table 2). Also, when the head rebounds, the vertical load on the head decreases and the compressive load at T1 increases as the negatively directed head velocity is opposed by the cervical spine (Fig. 6). Head rebound was further corroborated by the head acceleration data (Fig. 6). The maximum axial (or z) neck load due to head rebound was calculated from the difference between the z neck force and z head force. Rebound accounted for up to 963 ± 390 N in the padded impacts and 662 ± 428 N in the rigid impacts. This constituted as much as 54 ± 16 and $38 \pm 30\%$ of the total neck load for the respective surfaces. The difference between these percentages for the

Table 2. Kinetic data

Test	Head force resultants (N, ms)				Neck force (N, ms)		Impulse		Momentum		Peak Moment (Nm)	Lag† (ms)
	Mode 1		Mode 2		Resultant		Head	Torso	Head	Torso		
	Peak	Time*	Peak	Time*	Peak	Time*	Ns	Ns	Ns	Ns		
A	7938	1.6	4925	7.2	4189	8.8	-12.5	-46.9	11.0	38.8	57.2	1.5
B	8566	1.3	2759	6.9	2643	4.6	-13.0	-40.7	11.6	51.1	151.8	1.6
C	8111	1.4	4052	11.8	3010	10.7	-14.0	-47.7	12.6	52.1	98.0	2.1
D	11621	2.1	3282	7.4	2891	6.6	-21.1	-24.1	14.5	50.2	49.1	2.2
E	5615	1.8	3568	3.5	2079	9.1	-12.4	-22.4	10.0	52.3	115.6	1.3
F	7498	1.4	2705	8.8	2533	11.7	-12.2	-62.6	11.8	57.8	48.6	1.5
G	8790	1.3	1898	14.9	1971	12.8	-12.9	-32.4	12.1	51.6	77.0	1.8
H	1759	11.2	1461	26.6	1762	20.9	—	-42.7	—	50.0	-38.9	5.3
I	3627	16.6	1623	36.4	2128	34.6	—	-39.7	—	48.4	-77.8	5.8
J	3857	13.0	2844	24.5	2595	32.4	—	-31.7	—	56.0	-119.1	7.5
K	2604	16.2	1043	33.5	1289	45.0	—	-22.6	—	49.0	73.1	9.0

* Time of peak force (contact at time = 0 ms).

† The delay between head impact and onset of response at T1.

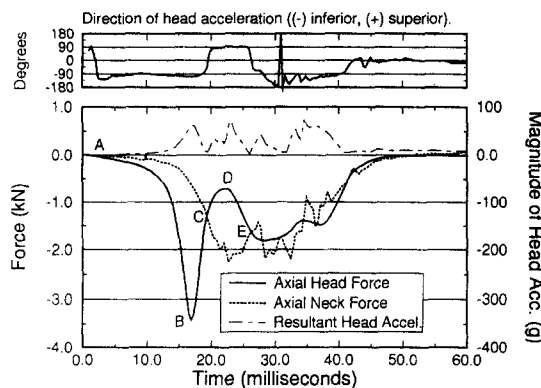


Fig. 6. Axial (z) head and T1 force histories for Test J illustrating rebound loading after the first mode in the head force. At point A, the head is subjected to a negative acceleration in response to the negatively directed impact force. The head center of gravity maintains a positive velocity until point B while the head (and padding) are axially compressed. The velocity of the head changes direction and the head begins to rebound. At C, the forces measured by the load cells at the head and at T1 are equal and the vertical acceleration of the head at point C must be 0 to satisfy dynamic equilibrium. This was corroborated by the head acceleration data. At point C, the head center of gravity is subjected to a positive acceleration as the cervical spine becomes loaded by the inertial force of the rebounding head. The vertical velocity of the head changes sign again at point D. At point E, much of the initial kinetic energy of the head has been dissipated and the effect of the head inertial force on the axial response is reduced. Between points C and E, the difference between the head force and T1 force is the neck force due to head rebound.

rigid and padded impacts was not significant using a two-sample *t*-test ($p > 0.3$). Cervical spine injuries occurred during the head rebound phase of neck loading in all the traumatic padded impacts (Figs 5 and 6). Rebound loading of the cervical spine was observed in all the padded impacts and in five of the seven rigid impacts. The remaining two of seven rigid impacts (D and E im-

pacting at -15°) escaped injury. The evidence for rebound in these two tests was not conclusive.

Dynamic buckling of the cervical spine was observed in these experiments regardless of surface type or orientation. In a column with a fixed base, buckling is evidenced by an abrupt decrease in measured compressive load with increasing deflection and moment (Fig. 7). Snap-through buckling (Chen and Lui, 1987) is characterized by a visible and rapid transition from one equilibrium configuration to another (Fig. 8, 4 ms). One or both of these hallmarks was observed in all the specimens tested. The deformation pattern of the post-buckled mode is shown schematically (Fig. 9) together with the injuries produced, and can also be seen in the high-speed image

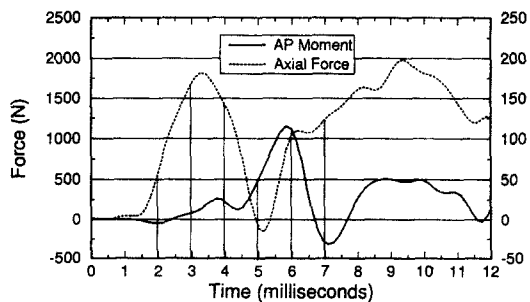


Fig. 7. Axial neck force and anteroposterior moment histories for Test E showing cervical spine buckling between 3 and 5 m. Each vertical line corresponds to a video frame in Fig. 8. Compressive force has a positive sign in this figure so that it may be more easily compared with the moment. During buckling, the cervical spine loses axial stiffness and the compressive load decreases. This results in a drop in the measured axial force (4 ms). Increasing eccentricity of the axial load, increasing shear, and cervical spine inertia give rise to flexion bending moments. Once the new equilibrium position is reached (5.5 ms), the axial load rapidly increases and reaches its peak value for the test. Note the tensile force at 5 + ms due to the inertia of the cervical spine. Test E had no cervical spine injury.

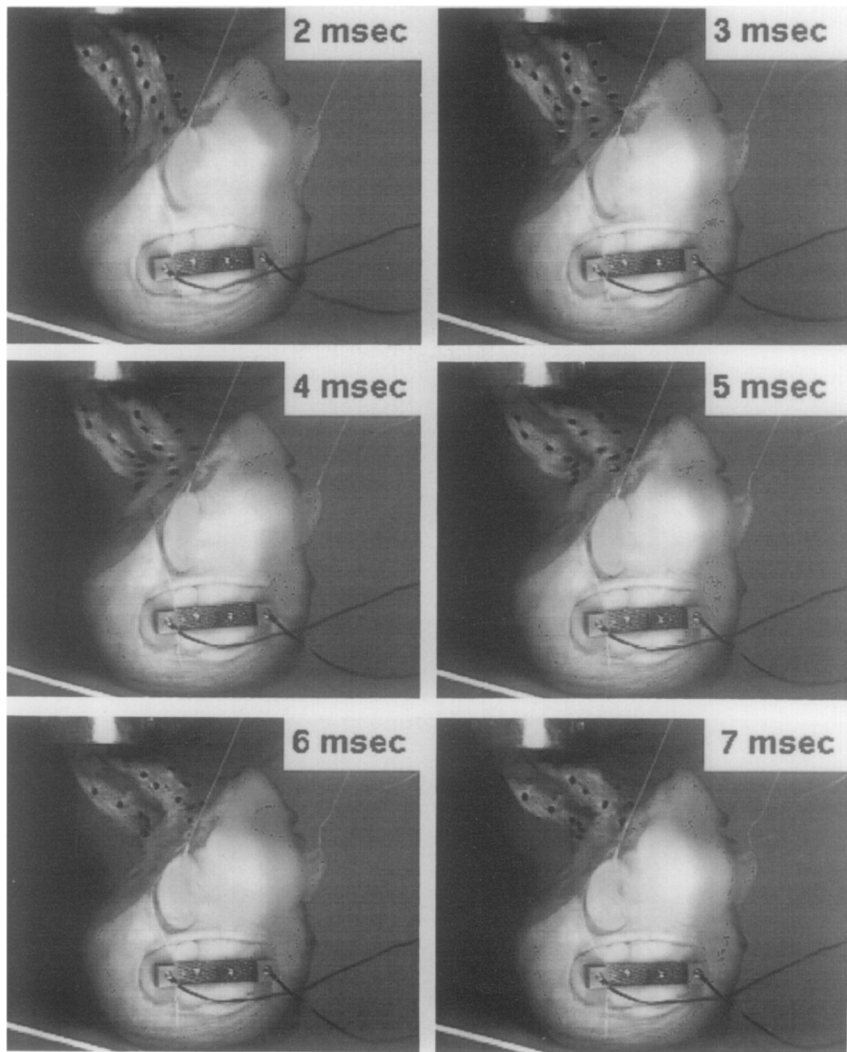


Fig. 8. Six frames of video data (Test E) illustrating cervical spine buckling. At 3 and 4 ms, the cervical spine snaps through to a new equilibrium position (6 ms) which is locally flexed at C6-T1 and extended at C1-C5. The force and moment histories for this test are shown in Fig. 7. Test E had no cervical spine injury.

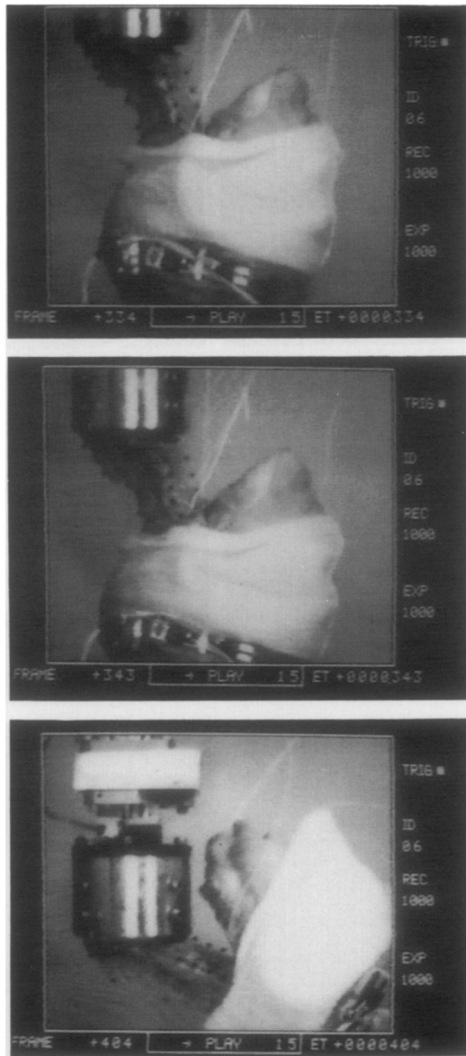


Fig. 10. An impact sequence illustrating a higher-order buckling mode. The initial position is shown in the first frame, 4 ms before impact. At 5 ms following impact the higher-order mode is observed. Subsequent head rotation of greater than 90° is shown in the last frame (66 ms after impact).

data [Fig. 8 (6 ms)]. It was characterized by extension with extension type injuries in the C3-C5 motion segments (C2-C3-C4-C5 and the connecting ligaments), and flexion with flexion type injuries in the C7 and C8 motion segments (C6-C7-T1) and the connecting ligaments. The buckle occurred 3-8 ms after impact and the resulting mode of deformation provides the mechanism for 14 of the 15 injuries produced in the C2-C7 vertebrae. The exception was specimen (G) which had a vertical compression injury at C3 in addition to distractive extension injuries at C3-C4 and C4-C5.

In four of the rigid impacts (D, E, F, and G), a transient, higher-order buckling mode of deformation was observed prior to the first-order mode described above (Fig. 8, 3 ms and Fig. 10). Two of these specimens escaped injury, and the other two sustained injuries later in the event. The unstable higher-order mode was observed

during the ascending portion of the neck loading curve, and lasted 2-8 ms.

DISCUSSION

Numerous investigations have demonstrated the importance of end conditions in cervical spine testing. However, there have been no studies which quantify the effects of head inertia on cervical spine loading and injury. This study explores these effects with the primary goal of determining whether the head inertia can generate a constraining cervical end condition. In addition, impact surface and orientation were varied to evaluate their effects on injury risk.

The primary limitation of this study is the inherent lack of active neck musculature in cadaver models.

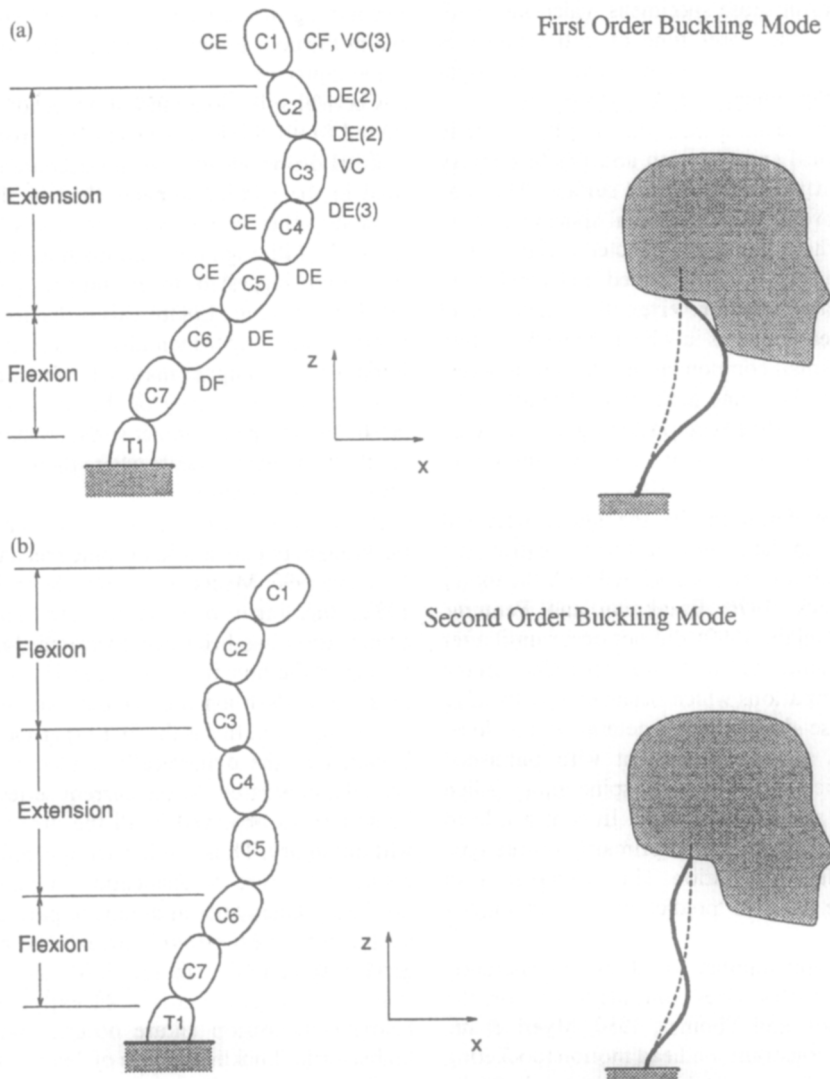


Fig. 9. (a) The first-order buckling mode showing the distribution by level of all the injuries produced and their relation to the local deformation at each vertebral motion segment. The fixed end represents T1 and the specimen cup. (b) The transient, higher order buckling mode.

Muscles undoubtedly play a role in stabilization and energy absorption during trauma; however, their importance is minimized during compressive loading. This was the rationale for limiting the tests to vertical impacts with the head, neck, and torso aligned in an anatomically neutral position. The results show that injury occurred two to three times quicker than the cervical spine muscle reflex, which further mitigates the role of musculature in these impacts. Previous studies report cervical spine muscle reflex times ranging from 50 to 65 ms (Foust *et al.*, 1971; Schneider *et al.*, 1975), which is considerably longer than the 20 ms required to produce injury in these experiments.

No attempt was made to normalize the impact energy based on the weight of the tissue donor. Instead, the mass of the effective torso, and the impact velocity were held constant. By doing so, the kinetic energy of the torso was nearly the same for drops of equal height.

Another limitation is our inability to determine the sequence of injuries in those specimens which had multiple failures. Only the onset time of initial injury is reported, with no distinction being made between propagation of the primary injury and secondary injury.

These experiments demonstrate that the head inertia can constrain cervical spine motion and produce injury in the absence of a pocketing impact surface. This was evidenced by the production of cervical spine injuries in the experiments where the head impacted a rigid, lubricated Teflon surface (an unconstrained end condition). This was particularly true for vertex (0°) impacts, and anterior ($+15^\circ$) head impacts in which the neck loading vector had only a small component in a direction necessary to accelerate the head and neck out of the path of the following torso. Thus, while head pocketing may increase cervical spine injury risk, it is not requisite for injury during impact.

As a consequence of head inertia, the injuries occurred prior to any significant head motion. The more dramatic head motions, which are often associated with the injury mechanism (Babcock, 1976; Braakman and Penning, 1971; White and Panjabi, 1990), did not occur until after injury. The type of injury produced was dependent on the cervical spine deformations which occurred shortly after head impact. These deformations determine the local injury mechanism and are consistent with published mechanistic classifications of cervical spine injury (Allen *et al.*, 1982; White and Panjabi, 1978). In contrast, head motion following injury depended primarily on the type of surface and surface orientation. Thus, observed head motion cannot be used to predict or classify impact injury.

While of insufficient number for statistical inference, the -15° impacts in this series continue to support the hypothesis (Hodgson and Thomas, 1980; Myers *et al.*, 1991) that physical constraint on head motion (pocketing of the head) can increase cervical spine injury risk. In the two -15° rigid impacts (D,E), the head and neck were able to flex out of the path of the torso and escape injury. In contrast, the padded -15° head impact (K) con-

strained the head in the foam surface for a sufficient amount of time to produce injurious neck loads. Specimen K sustained transverse tears of the anterior longitudinal ligaments and anterior discs at C2-C3 and C3-C4.

The decoupling between cervical spine and head has been reported previously (Pintar *et al.*, 1990) and is a consequence of the low initial stiffness in the load deflection curve of the spine (Oxland and Panjabi, 1992). Data from Liu *et al.* (1992) report as much as 12° of combined flexion and extension at O-Cl with less than 0.5 N m of moment. This laxity in the cervical spine and in the craniocervical articulation results in a bimodal characteristic for the head force which has been previously described by Nusholtz *et al.* (1981, 1983). In the rigid impacts, head loads had fallen to a local minimum prior to the development of significant neck loads. Therefore, the first mode impulse is associated with stopping the head, and the corresponding peak load is not indicative of the loads that the neck will experience. This decoupling in the head and cervical spine structure explains the poor predictive ability of head force on cervical spine injury risk.

Cervical spine loading due to head rebound was observed in all the injury producing drops and in all the padded drops. Head rebound accounted for more neck load in the padded impacts than in the rigid impacts; however, this result was not statistically significant ($p > 0.3$). Although rebound loading of neck by the head has been suggested from lumped parameter models (McElhaney *et al.*, 1983b), this is the first time it has been demonstrated experimentally. This result emphasizes the importance of impact materials which completely dissipate the kinetic energy of the head and suggests that elastic (undamped) contact surfaces should be employed carefully in environments where there is the potential for head and neck injury.

It has been suggested by a number of authors that buckling may play a role in spine mechanics (Crisco and Panjabi, 1990; Myers *et al.*, 1991; Schneider, 1973; Torg, 1982). Buckling from a compression to a flexion mode of deformation has been demonstrated during quasi-static testing in the human cadaver cervical spine at low compressive loads when the occiput was free (Myers *et al.*, 1991). However, this is the first experimental study where buckling in the dynamically loaded cervical spine has been demonstrated. In the current series of experiments, buckling was observed in all the drops, and sometimes without injury. Thus, while buckling does not necessarily result in fracture or dislocation, it plays a role in the pre-injury kinematics and may, in part, explain the basis for the poor relationship between head motion and local cervical spine injury. In addition, these findings indicate that the cervical spine is sufficiently slender to buckle before compression failure occurs, and that transient, higher-order buckling modes of deformation are produced during axial impact. It is recognized that passive muscle tone would increase the buckling load and possibly alter the modes of deformation due to the stiffening effects of the muscle itself, and the stiffening effect of

muscle loads on the ligamentous spine. The contributions of these buckling modes to cervical injury mechanics is a topic for further investigation.

All the injuries produced in this investigation have been observed clinically. Interestingly, six of the seven injured specimens had upper cervical spine injuries. The incidence of such injuries in survivors of cervical spine trauma has been reported to be as low as 20% (Burke *et al.*, 1985) and as high as 37% (Harrington *et al.*, 1986). However, Fife *et al.* (1986) report a 48% incidence in the survivors of motor vehicle accidents (MVA). The incidence is even higher in fatal MVAs. Epidemiological studies by Alker *et al.* (1975) and Buchholz *et al.* (1979) report greater than 50% incidence of upper cervical spine injuries in fatal MVAs. This might indicate that the vertical impacts in this study represent some of most severe, and potentially fatal, types of traumatic loading.

Of the five specimens with atlas (C1) injuries, four had additional injuries to the lower cervical spine. Levine and Edwards (1989) report a 53% incidence of additional cervical spine injury in surviving subjects with fractures of the arch of the atlas. Multiple noncontiguous injuries were also observed in the three specimens. Reports by a number of investigators suggest that multiple noncontiguous injuries occur with frequency of 10–20% in survivable cervical injuries, and are likely under diagnosed (Shear *et al.*, 1988). Thus, this sample of cervical injuries appears representative of population, supporting the validity of this injury model.

CONCLUSIONS

(1) Inertial loading of the neck by the head may be sufficiently large to produce a constraining head end condition in the absence of a pocketing impact surface. This effect is particularly evident in impacts in which the head has no velocity component tangent to the impact surface.

(2) Cervical spine loading due to head rebound was observed in all traumatic impacts tests. As a consequence of rebound, there are times when the forces on the cervical spine can be considerably greater than the measured head force.

(3) Observed head motions are not predictive of the local injury mechanism in impact injury.

(4) Dynamic structural buckling modes of the cervical spine were observed. The buckling modes may be transient and are not directly associated with injury. However, they alter the cervical spine kinematics, and may therefore influence the types of injuries which are produced.

Acknowledgements—This study was supported by the Department of Health and Human Services, Centers for Disease Control Grant R49/CCR402396-06, the National Disease Resource Interchange, and the Virginia Flowers Baker Chair.

REFERENCES

- Alker, G. J., Oh, Y. S., Leslie, E. V., Lehtotay, J., Ppanaro, V. A. and Eschner, E. G. (1975) Postmortem radiology of head and neck injuries in fatal traffic accidents. *Radiology* **114**, 611–617.
- Allen, B. L., Ferguson, R. L., Lehmann, T. R. and O'Brien, R. P. (1982) A mechanistic classification of closed indirect fractures and dislocations of the lower cervical spine. *Spine* **7**, 1–27.
- Babcock, J. L. (1976) Cervical spine injuries. *Arch Surg.* **111**, 646–651.
- Bauze, R. J. and Ardran, G. M. (1978) Experimental production of forward dislocation of the human cervical spine. *J. Bone Jt Surg.* **60-B**, 239–245.
- Brakman, R. and Penning, L. (1971) Causes of spinal lesions. *Injuries of the Cervical Spine*. Excerpta Medica Foundation, Amsterdam.
- Buchholz, R. W., Burkhead, W. Z., Graham, W. and Petty, C (1979) Occult cervical spine injuries in fatal traffic accidents. *J. Trauma* **19**(10), 768–771.
- Burke, D. C., Burley, H. T. and Ungar, G. H. (1985) Data on spinal injuries — I. Collection and analysis of 352 consecutive admissions. *Aust. NZ J. Surg.* **55**, 3–12.
- Cavanaugh, J. M. and King, A. I. (1990) Control of transmission of HIV and other bloodborne pathogens in biomechanical cadaveric testing. *J. Orthop. Res.* **8**, 159–166.
- Chen, W. F. and Lui, E. M. (1987) *Structural Instability: Theory and Implementation*, pp. 4–10. Elsevier, New York.
- Crisco, J. J. and Panjabi, M. M. (1990) Euler stability of the ligamentous human lumbar spine. *Proceedings of the 36th Annual Meeting of the ORS*, 607.
- Fife, D. and Kraus, J. (1986) Anatomic location of spinal cord injury: relationship of the cause of injury. *Spine* **11**, 2–5.
- Foust, D. R., Chafin, D. B., Snyder, R. G. and Baum, J. K. (1971) Cervical range of motion and dynamic response and strength of cervical muscles. *The 17th Stapp Car Crash Conference*, p. 285.
- Harrington, T. and Barker, B. (1986) Multiple trauma associated with vertebral injury. *Surg. Neurol.* **26**, 149–154.
- Hodgson, V. R. and Thomas, L. M. (1980) Mechanisms of cervical spine injury during impact to the protected head. *Proceedings of the 24th Stapp Car Crash Conference*, SAE Paper #801300, 17–42.
- Levine, A. M. and Edwards, C. C. (1989) Fractures of the atlas. *J. Bone Jt Surg.* **73**(5), 680–691.
- Liu, Y. K., Krieger, K. W., Njus, G., Ueno, K., Connors, M. P., Wakano, K. and Thies, D. (1982) *Cervical Spine Stiffness and Geometry of the Young Human Male*. Air Force Aerospace Medical Research Lab., AFAMRL-TR-80-138.
- McElhaney, J. H., Paver, J. G., McCrackin, H. J. and Maxwell, G. M. (1983a) Cervical spine compression responses. *Proceedings of the 27th Stapp Car Crash Conference*, SAE Paper #831615, pp. 163–177.
- McElhaney, J. H., Roberts, V. L., Paver, J. and Maxwell, M. (1983b) Etiology of trauma to the cervical spine. In *Impact Injury of the Head and Spine* (Edited by Ewing, C. L., Thomas, D. J., Sances Jr, A. and Larson, S. J.). C. C. Thomas Publishers, Springfield.
- McElhaney, J. H., Snyder, R. G., States, J. D. and Gabrielsen, M. A. (1979) Biomechanical analysis of swimming pool injuries. *Society of Automotive Engineers*, paper no. 790137, 47–53.
- Myers, B. S., Richardson, W. J., Doherty, B. J., Nightingale, R. W. and McElhaney, J. H. (1991) The role of head constraint in the development of lower cervical compression flexion injury. *Proceedings of the 35th Stapp Car Crash Conference*, pp. 391–400.
- Nusholtz, G. S., Huelke, D. E., Lux, P., Alem, N. M. and Montalvo, F. (1983) Cervical spine injury mechanisms. *Proceedings of the 27th Stapp Car Crash Conference*, SAE Paper #831616, pp. 179–197.
- Nusholtz, G. S., Melvin, J. W., Huelke, D. F., Alem, N. M. and Blank, J. G. (1981) Response of the cervical spine to superior-inferior head impact. *Proceedings of the 25th Stapp Car Crash Conference*, SAE Paper #811005, pp. 197–237.
- Oxland, T. R. and Panjabi, M. M. (1992) The onset of progression of spinal injury: a demonstration of neutral zone sensitivity. *J. Biomechanics* **25**, 1165–1172.
- Pintar, F. A., Sances, A. Jr., Yoganandan, N., Reinartz, J.,

- Maiman, D. J., Suh, J. K., Unger, G., Cusick, J. F. and Larson, S. J. (1990) Biodynamics of the total human cadaveric cervical spine. *Proceedings of the 34th Stapp Car Crash Conference*, SAE Paper #902309, pp. 55–72.
- Schneider, R. C. (1973) *Head and Neck Injuries in Football*. Williams and Wilkins, Baltimore.
- Schneider, L. W., Foust, D. R., Bowman, B. M., Snyder, R. G., Chaffin, D. B., Abdelnovr, T. A. and Baum, J. K. (1975) Biomechanical properties of the human neck in lateral flexion. *SAE Transactions*, 751156: 3212.
- Shear, P., Hugenholz, H., Richard, M. T., Russel, N. A., Peterson, E. W., Benoit, B. G. and DaSilva, V. F. (1988) Multiple noncontiguous fractures of the cervical spine. *J. Trauma* 28(5), 655–659.
- Torg, J. S. (1982) *Athletic Injuries to the Head, Neck and Face*. Lea and Febiger, Philadelphia.
- Walker, L. B., Harris, E. H. and Pontius, U. R. (1973) Mass, volume, center of mass, and mass moment of inertia of the head and head and neck of human body. *Proceedings of the 17th Stapp Car Crash Conference*, SAE Paper #730985, pp. 525–537.
- White, A. A. and Panjabi, M. M. (1990) *Clinical Biomechanics of the Spine*. L. B. Lippincott Company, Philadelphia.
- Yoganandan, N., Sances, A. Jr, Maiman, D. J., Myklebust, J. B., Pech, P. and Larson, S. J. (1986) Experimental spinal injuries with vertical impact. *Spine* 11, 855–860.